Measurement Science and
Technology

PAPER • **OPEN ACCESS**

A method for assessing the uncertainty of a secondary dynamic pressure standard using shock tube

To cite this article: Christophe Sarraf 2021 *Meas. Sci. Technol.* **32** 015013

OPEN ACCESS
IOP Publishing
Measurement Science and Technology
Meas. Sci. Technol. 32 (2021) 015013 (12pp)
https://doi.org/10.1088/1361-6501/aba56a

A method for assessing the uncertainty of a secondary dynamic pressure standard using shock tube

Christophe Sarraf

LNE/ENSAM-LMD, Ecole Nationale Supérieure d'ARTS ET METIERS, Paris 75013, France

E-mail: christophe.sarraf@ensam.eu

Received 5 April 2020, revised 30 June 2020
Accepted for publication 13 July 2020
Published 2 November 2020

Abstract

Pressures are often measured in fast transient regimes, even if the transducers are not calibrated in dynamic regimes. If the solutions proposed for primary calibration of the dynamic response of pressure sensors must be fully recognised, secondary methods are also needed to disseminate the standard to final users. A method for assessing measurement uncertainty, carried out by comparison with a reference transducer, traceable to primary standard, is proposed here. A typical application is gas pressure measurement. This paper follows and supplements the work done on the Mach number method in 2018. For this work the reference transducer is calibrated by the 'collective standard method' currently used in the *'Laboratoire de Métrologie Dynamique'* (LNE/ENSAM). This primary standard uses steps of pressure as inputs for dynamic pressure calibration that are generated by shock tubes (STs) and fast-opening devices (FODs). The uncertainty on dynamic sensitivity is evaluated from the quasi-static to the low, medium and high-frequency range (up to 10 kHz) using bandwidth comparisons. To calibrate a secondary standard transducer in gas, the method also requires one or two step generators: an ST for high-frequency range calibration and a FOD for the low-frequency range. Concerning the main results of this paper, the transducer to be calibrated and the reference transducer are placed symmetrically on the endplate of an ST. The amplitude of the pressure step generated by the tube is used to excite the transducers. Finally, the uncertainty on the sensitivity in dynamic conditions is determined by comparison with a model expected to be exhaustive. The results are provided as an uncertainty budget assigned frequency by frequency. The question asked in this work concerns the measurand used in secondary calibration: can a pressure step generated by a non-ideal ST be used in the process of calibration by comparison, i.e. for a secondary dynamic calibration? A method is proposed. Since the secondary method is derived directly from the primary one, this paper recaps the primary dynamic calibration method in gas and the budget of the associated uncertainty. Then the paper presents a secondary method and options to overcome the principal default identified in the ST frequency range, namely the non-uniform pressure fields existing in the tube.

Keywords: dynamic pressure calibration, shock tube, secondary method, collective standard method, uncertainty evaluation

(Some figures may appear in colour only in the online journal)

Nomenclature

FOD	Fast-opening device
LMD	Dynamic Metrology Laboratory
ST	Shock tube
FRF	Frequency response function

1. Introduction

Manufactured products often have dynamic functional characteristics which must be controlled by accurate measurement. There is a need for dynamic calibration. Astronautic devices encounter small variations of pressure at frequencies whose order of magnitude extends up to several tens of kHz. If it is possible to ensure the traceability of static parameters such as sensitivity, the offset and the hysteresis, in most cases the dynamic characteristics of the transducer are not traceable.

The transducers have to be characterised dynamically and the ISA guide S37 [1] recalls the parameters of interest. Damion [2] proposed a primary method, inspired by the recommendations of Schweppe *et al* [3]. The details of the uncertainty evaluation are not published. Hjelmgren in 2002 [4] stated the need for primary and secondary dynamic calibration standards and pointed out the lack of existing methods to cover large ranges in pressure and frequency bandwidth, in particular the lack of traceability. Olivera [5] for his PhD thesis fully developed the primary method. A brief state of the art of gaseous dynamic calibration applications was recalled by Sarraf and Damion in a previous work on the primary Mach number method [6].

To support industrial needs for traceable calibration in dynamic pressure applications, European National Metrology Institutes (NMIs) are developing new primary and secondary measurement standards especially in the 17IND07 DYNPT European project [7]. In that context, for low pressures in gas which range from 0.01 to 10 bar and frequencies from quasi-static to 10 kHz, LNE/ENSAM improved its primary dynamic calibration standard using fast-opening devices (FODs) and shock tubes (STs) and developed a method using a reference transducer to calibrate secondary transfer standards and working standards. The methods and techniques are presented in this paper.

1.1. Calibration equipment generally used for gaseous applications

1.1.1. Generators. Schweppe *et al* [3] review the types of generators existing for dynamic calibration in gas. Aperiodic generators are used to generate dynamic pressure input exiting systems over large frequency ranges [8].

Two types of step generators used for dynamic pressure calibration in gaseous media are considered in this communication: the FOD and the ST.

1.1.1.1. FODs. The transducers are excited in the frequency range from quasi-static to few hundreds of Hertz by the steps of pressure generated by the FOD. Schweppe *et al* remind that the best FODs known have a rising time in the order of 0.25 ms [3].

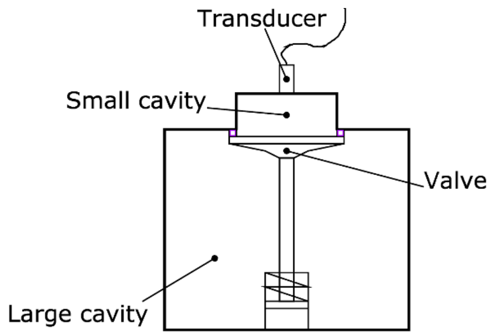

Figure 1. Synoptic scheme of an FOD and pressure step generated.

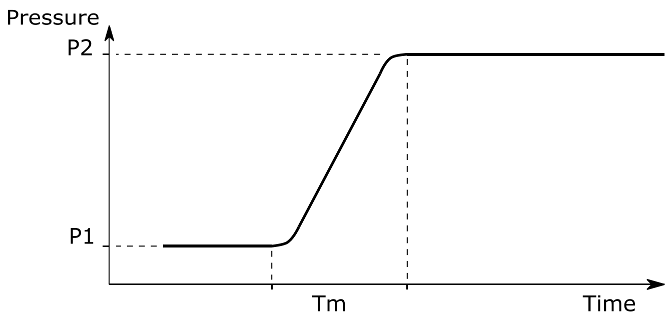

Figure 2. Diagram of a theoretical pressure step generated by an FOD.

The type of FOD used at LNE/ENSAM to calibrate the reference transducer is a fast-opening valve represented schematically figure 1. The high-pressure large cavity is inflated to pressure P2. The volume of this cavity is much larger than that of the low pressure inflated to P1. The ratio of volumes is in the order of 10^4. The valve is driven by a pneumatic jack filled with helium for a quick emptying. The reference sensor to be calibrated is mounted on the smallest cavity.

Due to the large difference between the volumes of the two cavities, the pressure in the volume after opening is not significantly different to P2. This makes the amplitude of the step traceable in the static regime. The step of amplitude $\Delta P = P_2 - P_1$ is generated and represented schematically figure 2. Its rising time T_m isabout 0.25 ms when operated in standard conditions.

The rising time is short but, due the small amplitude of the steps chosen in the protocol of calibration to limit the effect of acceleration and temperature, the spectral content of the input is not sufficient to excite the transducers beyond 1 kHz. For primary calibration, which considers that the FOD generates a perfect step, the imperfections are no longer acceptable after 100 Hz.

Moreover, Razzak *et al* [9] remind that special attention has to be paid to transducers not passing the continuous component. The amplitude of the output cannot be accurately determined directly due to its ongoing decay during the rise of the

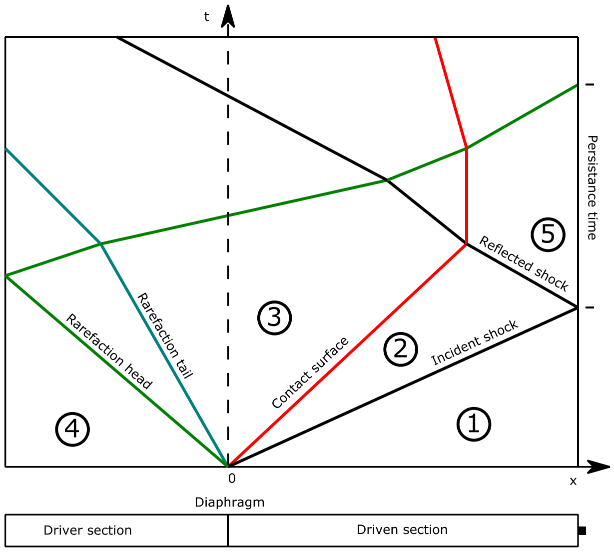

Figure 3. Outline of shock propagation in a theoretical ST.

input. In that case the calibration has to be made by comparison following an appropriate protocol.

1.1.1.2. STs. This equipment is widely developed for its ability to generate strong temperature and pressure steps and used to produce chemical reactions [10–13]; for pressure calibration it is used differently: recently STs have been used in calibration as a step generator [14] or high-pressure quasi-pulse generator [15]. At LNE/ENSAM, STs are used to generate the aperiodic inputs for primary calibration in the range from 25 Hz to 10 kHz. The ST must generate a step of pressure of small amplitude, in the order of a few percent of the range of the transducer, and with as small temperature rise and acceleration as possible. The order of rising time of the step is much less than a microsecond; however, imperfections in the generated step limit the calibration range of frequency. Sarraf and Damion [6] recall references to the theory and Hanson *et al* [13] the limitation of the STs. Conditions are set to produce a step as close to the theoretical one as possible. Figure 3 represents the space-time diagram of the ST. Sections are separated by a diaphragm and inflated at different pressures. The driver section is inflated at high pressure and the driven section at low pressure respectively in condition 1 and 4. These chambers can be filled with different gases for particular optimisations [13].

After the burst of the diaphragm, the compression waves focus and create a shock. The shock wave propagates into the driven chamber at a speed superior to the speed of sound in the undisturbed media. Behind this singularity the pressure is equal to P2 and rises to P5 after reflection from the endplate. This wave is followed by the contact surface, i.e. the interface between the driver and the driven gas. It moves slower in a translation process with density and temperature discontinuity. The shock wave, which is reflected on the endplate, encounters the contact surface on its way back. This interaction can cause partial reflection of the wave which moves again toward the endplate and affects the quality of the step which is no longer as close as possible to the perfect step. The effects of rarefaction waves are complex; only the first incident shock is used for calibrations. If the initial conditions are defined to produce environments where the acoustic impedances are almost equal on both sides of the contact surface, this reflection will not be significant. In that case the conditions are said to be ‘tailored’. In dynamic calibration procedures the quasi-tailored condition is achieved by lowering the initial pressure ratio which must be less than 1.5. Otherwise in special dynamic characterisation, the signal is discarded after the arrival of the phenomenon. A much more complicated technique for achieving quasi-equal acoustic impedances is to use mixtures of different gases [13].

Sarraf and Damion [6] recalls the causes of restrictions on the use of STs for dynamic pressure calibration. They are firstly due to the defaults induced by the diaphragm curvature as [16] shows. This paper also shows that transducers are sensitive to acoustical transverse modes of the tube when they are not placed in the centre of the endplate.

2. Calibration methods

Since the object of this paper, the secondary method, is derived directly from the primary method, the latter is recalled first.

2.1. Collective standard primary method

The objective of the primary dynamic pressure collective standard is to establish a defined relationship between the pressure and the measurement in the frequency domain. At the start of the process, the pressure is conventionally defined as a force over a surface with traceability to primary static pressure standards. The last major developments on the collective standard method were carried out by Olivera [5] and since then there have been continuous technical improvements.

2.1.1. Primary standard equipment and process. The dynamic reference for the primary standard is a dematerialised ideal step. The generators of the steps of the collective dynamic standards used for this work are sketched in figure 4, and figure 5 is the corresponding picture. They are built and used according to procedures to produce pressure steps as ideal as possible; and at the end, the effects of the real steps increase the uncertainty of measurement of the reference transducer calibrated. Primary dynamic calibration begins by quasi-static calibration of a transducer by comparison following a classical method. A manometer is used and the amplitudes of steps generated by the FOD are traceable to the International System of Units (SI) in this way. So this standard is called primary because it is maintained by a National Metrologic Institute (LNE) via a Delegated Institute (ENSAM).

The differences between the measurement and the pressure rapidly varying, the measurand, are not only due to the transducer itself but also to all the constituent parts of the chain of measurement, settings and analyses. This is why the reference is calibrated with its chain: a transducer selected for its intrinsic dynamic qualities, an amplifier, an analogic filter, a transient recorder and a signal analysis unit.

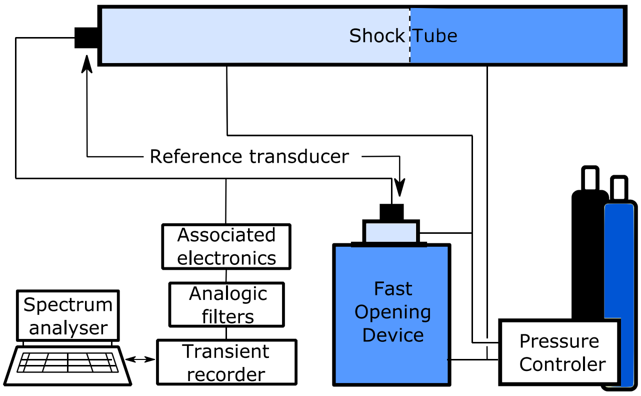

Figure 4. Equipment involved in the calibration process of the primary collective dynamic pressure standard.

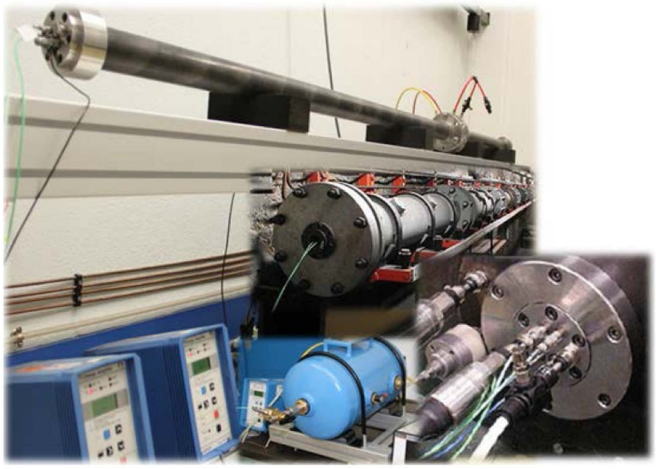

Figure 5. Step generators involved in the process of calibration of the primary and secondary collective dynamic standard. From top to bottom: TCHF 10 bar (high-frequency range), TCR 10 bar (medium-frequency range), FOD 20 bar (low-frequency range), FOD 16 bar (quasi-static).

The primary method consists of calibrating firstly in the quasi-static regime then in the dynamic regime all the subsets of the chain that are not already traceable from SI. An assessment of the uncertainties attributable to each of the inputs involved in the process is obtained; more particularly the uncertainty of the dynamic sensitivity of the voltage acquisition chain and of the dynamic sensitivity of the pressure transducer.

As an illustration, the results of measurement of typical pressure steps generated by the 'Tube à Choc de Référence' (TCR), the 23 metre long ST of LNE/ENSAM, are shown in figure 6. Outputs come from the KISTLER 601A sensor mounted flush on the endplate of the TCR; the media is air at ambient temperature.

2.1.2. Principle of primary standard method and uncertainty evaluation. The primary method consists of considering an

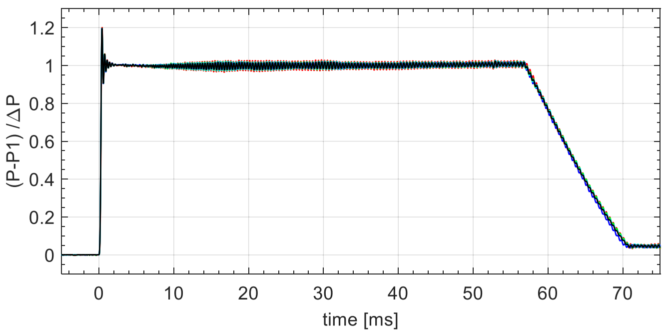

Figure 6. Example of pressure steps measured on the TCR endplate by a piezoelectric sensor; the TCR is an ST 23 metres long. Four normalised pressure steps are plotted, superimposed with their average.

ideal pressure step of amplitude $\Delta P = (P_2 - P_1)$ as input. This ideal step is the reference in the calculation of the frequency response function (FRF) of the system where the output is the measurement. The measurement at this stage is only traceable in the quasi-static domain, i.e. only P_1 and P_2 are traceable. The functional relationship of the ideal step is shown in equation (1), where $\boldsymbol{\theta(t)}$ is the Heaviside step function.

$$\Delta P = Y(t) = (P_2 - P_1) \cdot \theta(t). \tag{1}$$

The actual step produced by the ST is measured by the reference transducer; the associated functional relationship is given by the time-dependent equation (2) where ΔU_{ref} is the dynamic voltage measurement, S_{ref} the quasi-static sensitivity of the transducer and G_{ref} its dynamic gain. For the convenience of the presentation of the method, the dynamic sensitivity of the transducer is expressed by the product $S_{ref}{*}G_{ref}$. An important point is that for primary calibration, in principle, G_{ref} is set equal to one. The dynamic uncertainty will result from the differences that appear between this reference gain and the FRF gain calculated from the measurement.

$$\Delta P_{ref} = \frac{\Delta U_{ref}}{S_{ref} * G_{ref}}. \tag{2}$$

Not all the intermediary measurands and models of the process could be detailed in the format of this paper. In the preliminary sequences of quasi-static and dynamic calibration of the acquisition system, the measurands consist of voltage steps. At ENSAM the dynamic voltage calibration process is similar to the pressure one, using steps generated by a reference voltage generator. The full description of the method is addressed in Olivera's PhD thesis [5].

2.1.2.1. Uncertainty sources. Frequency by frequency, the uncertainty on the dynamic pressure measurement is evaluated, taking into account the sources presented in figure 7. The parameters which are not directly functionalised inputs are represented in the dashed box; the associated uncertainty is taken into account globally by the experimental deviation ε(B2). The main divergences from the Rankine–Hugoniot

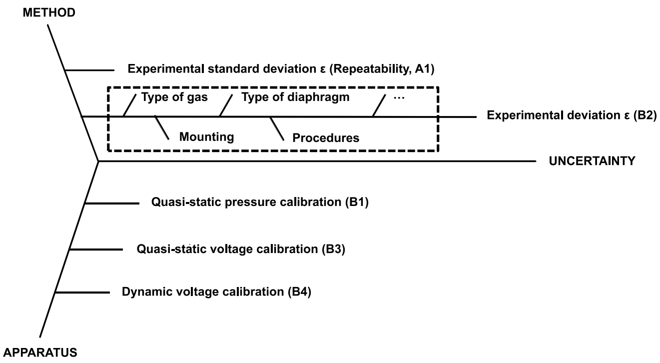

Figure 7. Sources of uncertainty taken into account during the last step of dynamic primary calibration of a pressure sensor, according to the collective standard method.

model [17] attributable to these parameters seem fairly repeatable. If their origins are identified the effect of these phenomena cannot however be functionalised in amplitude. In primary calibration, the limiting defaults are essentially due to oblique shock waves generated after the burst of the diaphragm separating the two chambers of the tube. Daru and Damion [16] showed the phenomenon due to a diaphragm initially curved. The other identified defaults are boundary layer effects, the progression of shock waves in media whose conditions are said to be non-tailored [17] and the effects of imperfections in the shape of a real tube. The temperature and vibration effects remain under control following the protocol. As an ideal step is considered as the reference these defaults increase the final uncertainty budget. The principle of the method is explained in the next paragraph:

In the final sequences of dynamic pressure calibration, the functional relationship of the measurand Y_+ is given by equation (3). In the relationship, the term *ε(t)* represents all the differences between the real step and the ideal step to take them into account in the model:

$$Y_+(t) = (P_2 - P_1) \cdot [\theta(t) + \varepsilon(t)]. \tag{3}$$

The FRF is the ratio of the Fourier transforms of the measurement relationship Y_+ over the reference Y, the latter corresponding to the perfect step from Rankine–Hugoniot theory.

$$H_{(f)} = \frac{\int_{t_0}^{+\infty} Y_+(t)\, e^{-2\pi j f t} dt}{\int_{t_0}^{+\infty} Y(t)\, e^{-2\pi j f t} dt}. \tag{4}$$

In practice, the continuous output is approximated by a series of steps or segments connecting discrete time measurements in the computation process of discrete Fourier transform (DFT). The DFT formulation is not presented here for convenience but its computations follow the methods recalled in the general case by Oppenheim and Schafer [18] and by Schweppe *et al* [3] for the particular step case. The uncertainty induced by DFT approximation is estimated in a black box approach from typical second-order theoretical inputs. Betta *et al* [19] proposes an alternative but much more complex method called 'white box', also compatible with the requirement of the Guide to the expression of Uncertainty in Measurement (GUM). As an alternative Yao *et al* [12] used discrete cosine transform and empirical mode decomposition to analyse the frequency content of the steps.

Observing the continuous formulation (4) with (1) and (3) it can be noted that for an evaluation of *ε(f)* the steps can be preliminary normalised (i.e. reduced by ΔP). Steps varying from mean initial value 0 to final value 1 are thus obtained. In practice, only one dynamic calibration is performed in the middle of the calibration pressure range. After that the reduced uncertainties are rescaled to the ΔP corresponding to the full range of calibration (here $\Delta P = 5$ bar in the calibration range). The transducer response is therefore considered linear in this range. This is the case for such high-quality transducers, chosen as a reference, when they are operated flush-mounted in this range of pressure.

The DFT computation begins at t_0 defined on the output signal. Discrepancies in t_0 lead to a phase lag that is the subject of future improvement of the model using shock detector inputs.

In the frequency domain, the uncertainty associated with the discrepancies *ε(f)* is evaluated as type B with a rectangular distribution as suggested by GUM. The standard deviation of $\varepsilon(f)$ is taken into account as an uncertainty of type A to take into account repeatability.

2.1.2.2. Technical considerations. A single dynamic measurand is not sufficient to perform the calibration over the entire frequency range, from quasi-static to high frequencies, because STs produce pressure steps that are too short in time. A first low-frequency pressure step is generated by an FOD. As the rising time of the FOD is long and its frequency range limited, the calibration continues on an ST. The measurands from the different generators necessary for the full calibration of the sensor have common frequency ranges which are used to establish cross-comparisons. The TCR long ST produces a measurand exiting the transducer down to 20 Hz. Unfortunately, STs produce detrimental pressure fluctuations, firstly due to the bursting of the diaphragm which has a curvature. The frequency of this default depends on the diameter of the tube [16]. For this reason, the TCR which has a large diameter of 200 mm is only used up to 1 kHz for primary calibration; the calibration continues on a smaller ST ('Tube à Choc Haute Fréquence' (TCHF)) to reach frequencies up to 10 kHz. Each generator corresponds to a sub-range of frequency and the acquisition chain settings are adapted according to these. These settings are defined in the calibration protocol.

The calibration carried out in a lower frequency range is used to make traceable the measurements of the boundary conditions carried out in a higher frequency range, that is to say to make traceable the measurement of P2 or P5 at the end of the step.

Figure 8 shows the steps and their inter-dependencies in the process of assessing uncertainties in the quasi-static, low, medium and high-frequency sub-ranges to reach 10 kHz. A manometer and a voltmeter measuring respectively the static pressure and the static voltage ensure traceability to national standards.

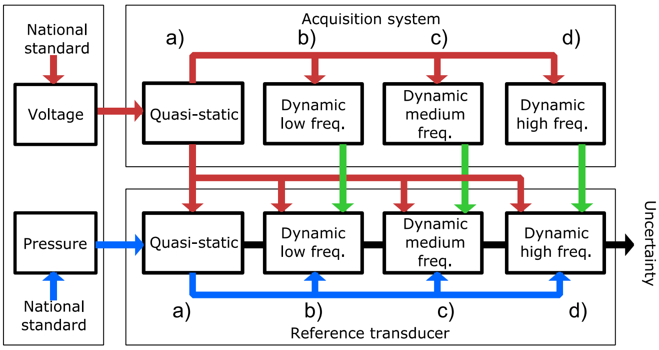

Figure 8. Schematic representation of the process followed in the evaluation of uncertainty in the collective dynamic pressure standard. Adapted from [6]. Four calibration steps (a, b, c and d) are necessary to ensure traceability to static national references at high frequency, both in pressure and in voltage.

2.1.2.3. Uncertainty model for primary standard calibration. The model used for the evaluation of the measurement uncertainty resulting from the primary calibration of a reference transducer is given in equation (5); the definitions and the hypothesis below are proposed:

$$u^2{}_{\Delta P_{ref}} = \left(\frac{1}{S_{ref} * G_{ref}}\right)^2 u^2{}_{\Delta U_{ref}} + \left(\frac{\Delta P_{ref}}{S_{ref}}\right)^2 u^2{}_{S_{ref}} + \left(\frac{\Delta P_{ref}}{G_{ref}}\right)^2 u^2{}_{G_{ref}} \tag{5}$$

- quasi-static sensitivity S_{ref} is constant
- the dynamic gain G_{ref} is stated at 1, and the dynamic uncertainty $u_{G_{ref}}$ is determined from the difference between the calculated gain and the theoretical gain equal to 1 (i.e. from the difference between the measured dynamic response and the perfect response)
- Input quantities are uncorrelated

In equation (5) we find the components of the uncertainty budget already presented graphically in figure 7 and defined below as B1, B2 and B4:

- B1: $u_{S_{ref}}$, quasi-static uncertainty in pressure
- B2: $u_{G_{ref}}$, dynamic uncertainty of gain in pressure
- B4: $u_{\Delta U_{ref}}$, dynamic uncertainty of acquisition system

To complete the budget the components A1, B3 and B6 have to be added; they are defined below:

- A1: repeatability
- B3: $u_{S_{T\_ref}}$, quasi-static uncertainty of acquisition system involved in B4
- B6: processing uncertainty involved in B4

Figure 9 shows the amplitudes of the FRFs based on ideal inputs and obtained according to the theoretical equation (4). The discrepancies from ideal responses obtained in the three ranges of frequencies with three different generators are plotted in different colours. The significant rise observable after

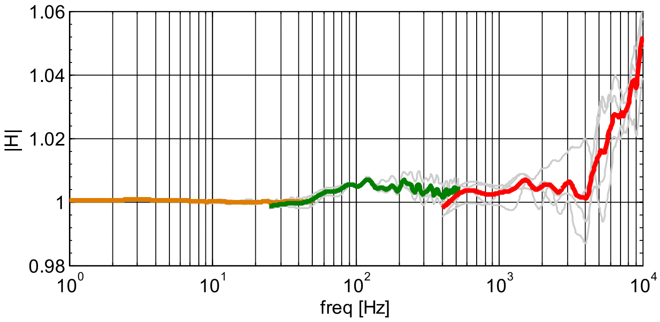

Figure 9. Amplitude of FRFs based on ideal inputs and overlap frequency bandwidth of the generators. The curves in colours are the average of the four FRFs plotted in grey in each bandwidth. FRF from FOD is in orange, from TCR in green and TCHF in red. The curves give an example of discrepancies from the ideal responses obtained on the primary standard with a piezoelectric transducer.

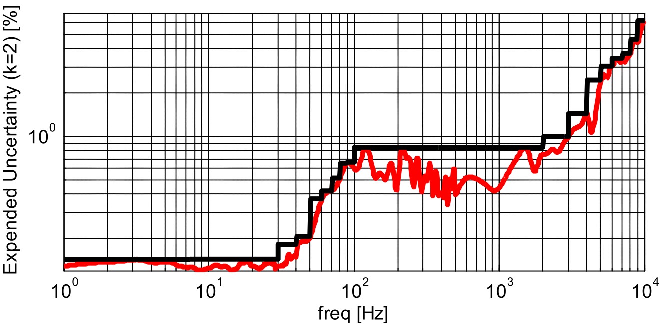

Figure 10. Example of extended uncertainty budget (k = 2) obtained at 5 bar pressure range gauge pressure. Raw data are plotted in red. The final results retained for the calibration certificate, corresponding to the highest value recorded in sub-frequency ranges, are plotted in black.

4 kHz corresponds to the effect of diaphragm curvature identified by Daru and Damion [16]. The corresponding fluctuation mode is close to 13 kHz. A new ST is developed as part of the 17IND07 project to reduce this default. Figure 10 shows an example of a final uncertainty budget obtained with a KISTLER 601A. The final results are established from the highest values recorded every 10 Hz, 100 Hz and 1000 Hz depending on the range.

2.2. Secondary method: comparison method

The main subject of this work, a secondary reference transducer, is now calibrated from the primary reference sensor. The method proposed is also suitable for calibrating working standards. There are a few differences in principle between the primary and secondary methods. They appear in the process. The main difference comes from the fact that in the case of secondary calibration the input is traceable in dynamic thanks to the reference transducer used in the comparison. So *a priori*, the generators could be ordinary if the pressures generated at the location of each of the two transducers are not significantly different. This paper shows that this is of course not always the case. However, the effect of the first significant pressure field

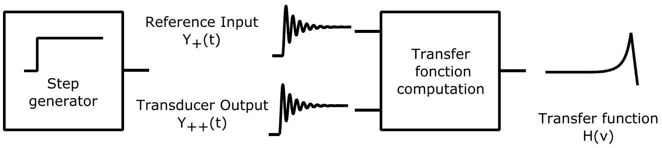

Figure 11. Schematic representation of the measurements involved in the calibration by comparison. The FRF calculation is used in the process of evaluating the experimental deviation from the reference measurement.

default, observed endplate of the ST , can be made not observable in the calibration.

2.2.1. Principle and model. The dynamic reference input is a pressure step; its measurement is traceable with a reference transducer and its associated chain. The output is the signal from the transducer to be calibrated associated with its chain of measurement. The FRF is computed on the basement of the step measured by the reference transducer; figure 11 shows the process schematically.

The functional relationship of the real step of pressure, the input Y_+ is given by the previously seen equation (3). For the output Y_{++} the relationship is given by equation (6) where the effects of all the discrepancies from the input are regrouped in the term $\xi(t)$ in order to be taken into account in the model:

$$Y_{++}(t) = (P_2 - P_1) \cdot [\theta(t) + \varepsilon(t) + \xi(t)]. \tag{6}$$

The FRF is the ratio of the Fourier transforms of the output step Y_{++} over the reference Y_+ as input given by equation (7).

$$H_{(f)} = \frac{\int_{t_0}^{+\infty} Y_{++}(t)\, e^{-2\pi j f t} dt}{\int_{t_0}^{+\infty} Y_{+}(t)\, e^{-2\pi j f t} dt}. \tag{7}$$

The step of amplitude ΔP_c in output is measured by the transducer to be calibrated according to the relationship given by the time-dependent equation (8), where ΔU_c is the dynamic voltage measurement, S_c the quasi-static sensitivity of the transducer and G_c its dynamic gain. For secondary calibration G_c is also stated to one as G_{ref} is stated to one for a primary calibration, and the model is similar to equation (5) used for primary calibration, where the subscript *ref* is replaced by *c*. The dynamic uncertainty u_{Gc} will result from the differences noted between this reference gain and the computed gain of the FRF. Note that the dynamic sensitivity S_c*G_c will only be expressed for the calibration of working transducers. In that case G_c could be different from one but it is not the subject of this paper. As the amplitude of the input step, ΔP is defined according to the relationship (9), the final model for uncertainty assessment is expressed by equation (10), where the input uncertainty $u_{\Delta P_{ref}}$ is taken into account.

$$\Delta P_c = \frac{\Delta U_c}{S_c * G_c} \tag{8}$$

$$\Delta P = \Delta P_{ref} \tag{9}$$

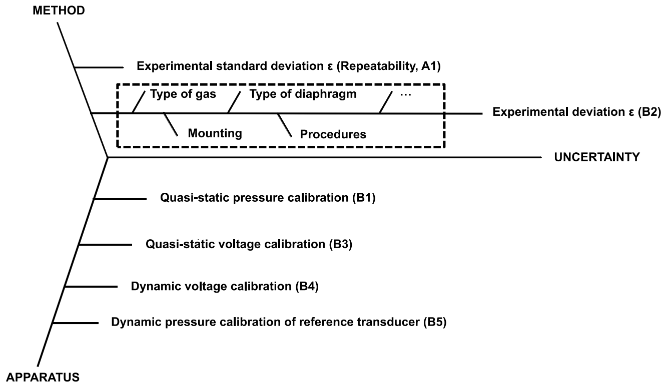

Figure 12. Sources of uncertainty taken into account during the last step of dynamic secondary calibration of a pressure sensor, according to the comparison method.

$$u^2{}_{\Delta P_c} = \left(\frac{1}{S_c * G_c}\right)^2 u^2{}_{\Delta U_c} + \left(\frac{\Delta P_c}{S_c}\right)^2 u^2{}_{S_c} + \left(\frac{\Delta P_c}{G_c}\right)^2 u^2{}_{G_c} + u^2{}_{\Delta P_{ref}}. \tag{10}$$

The budget components are presented in figure 12 and expressed below:

- B1: u_{S_c}, quasi-static uncertainty in pressure
- B2: u_{G_c}, dynamic uncertainty of gain in pressure
- B4: $u_{\Delta U_c}$, dynamic uncertainty of the acquisition system
- A1: repeatability
- B3: $u_{S_{T\_c}}$, quasi-static uncertainty of the acquisition system; involved in B4
- B6: processing uncertainty; involved in B4
- B5: $u_{\Delta P_{ref}}$, dynamic uncertainty of the input

3. Technical method, results and limitations

For the example presented, measurements are carried out on the reference ST of 2.25 metres long at LNE/ENSAM. This tube called TCHF dev2.0 is in development as part of the European project 17IND07. The performance of this tube in its use for secondary calibration is being improved. The reference transducer of the first chain of measurement, Chain 1, is used to ensure the traceability of the dynamic measurement. It has been previously calibrated on the primary standard using the collective standard method. The transducer of Chain 2 is calibrated according to the secondary method, and is called the 'by comparison' method. The two transducers are piezoelectric and of the type KISTLER 601A. The characteristics of the equipment used in the generator and in each of the calibration chains are listed in table 1.

The inner shape of the tube is modified to create a default and to analyse its effect on the calibration by comparison. This defect is a hollow ring corresponding to a local increase in the internal diameter of the tube.

3.1. Time measurement

The transducers are placed on the endplate of the driven section. The initial pressures P1 and P4, as defined previously

Table 1. Experimental setup.

	Device	Input/parameter
Step generator	Shock tube TCHF dev2.0	1–10 bar, Φ35 mm
	Driver section	0.75 m
	Driven section	1.50 m
	Diaphragm	Cellophane 21 µm (300P)
	Default: inner hollow ring	Φ_{ext} = 62 mm, Length = 3.5 mm
Gas	Air	Ambient compressed
Manometer	CPG 2500/10 bar	P1
Chain 1		*Reference transducer*
Pressure transducer	KISTLER 601B	Piezoelectric
Charge amplifier	KISTLER 5011B	TC, Long
Analogic filter	Kemo	40 kHz, Butterworth
Transient recorder	HBM Genesis	1 MHz
Chain 2		*In calibration*
Pressure transducer	KISTLER 601B	Piezoelectric
Charge mplifier	KISTLER 5011B	TC, Long
Analogic filter	Kemo	40 kHz, Butterworth
Transient recorder	HBM Genesis	1 MHz

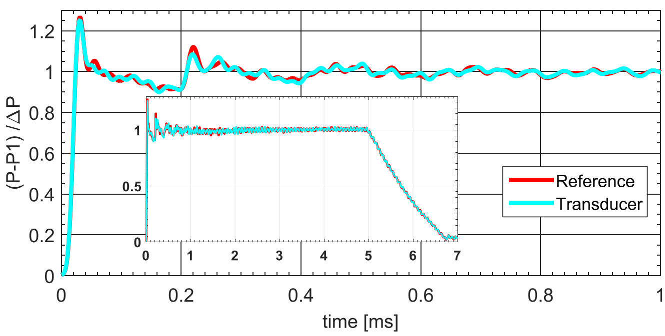

Figure 13. Example of pressure measurements on the TCHF endplate. Main plot shows the defaults of the steps and the differences between the input and output measurements. The insert shows the entire persistence time of this first incident step produced by the tube. The initial pressure P1 is set at 2 bar and P4 at 3.5 bar gauge pressure; the temperature is ambient.

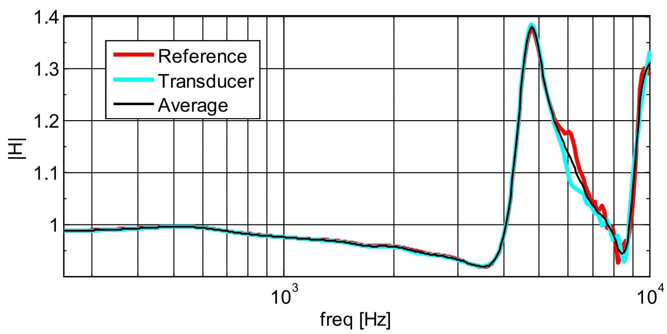

Figure 14. FRFs of each measurement based on an ideal step. A pick of amplitude appears close to 4.5 kHz due to the internal geometric default which was created for this work. Unexpected differences of amplitude appear around 6 kHz; the average 'smooths' them.

in figure 3, are set respectively at 2 bar and 3.5 bar gauge pressure. Under these conditions the diaphragm is close to the state of natural burst stress; the shock propagates in environments whose conditions are quasi-tailored; the rise in temperature has no significant influence since the Mach number of the initial shock is close to 1.1; it is checked that accelerations measured near the sensor are not significant on the basis of the specifications given by the manufacturer. Figure 13 shows the responses of the two transducers in the time domain. It is observed that the shape of the step is quite far from perfect; however, it should not be a problem for the process of calibration by comparison if the transducers are subjected to the same pressure.

3.2. Frequency domain

The defaults of the steps are first analysed from the FRFs calculated on the basis of a perfect step. The results are shown in figure 14. First an amplification peak appears for the spectral components at frequencies close to 4.5 kHz. This defect is due to the geometrical alteration created inside the tube for this work; for that a hollow ring is created in the driver section, located at 35 mm behind the diaphragm; the inner diameter of the tube is increased from 35 mm to 62 mm over a length of 3.5 mm.

Another default natural appears at around 6 kHz. Figure 14 shows that an excess of amplitude appears on one transducer when one deficit appears on the other at the same frequency which produces oscillations. These defaults are symmetrical with respect to the average of the two FRFs; when the average is calculated between the two FRFs, the result no longer exhibits these oscillations and therefore the average 'smooths' the amplitude oscillations. When unusual defaults appear in the dynamic measurement, the first point to check is the influence of the accelerations produced by the shock and undergone by the sensors. According to ISA 37 [1] recommendations, the principal check is to mount the sensors blinded to detect this effect. The measurement by an accelerometer (not presented

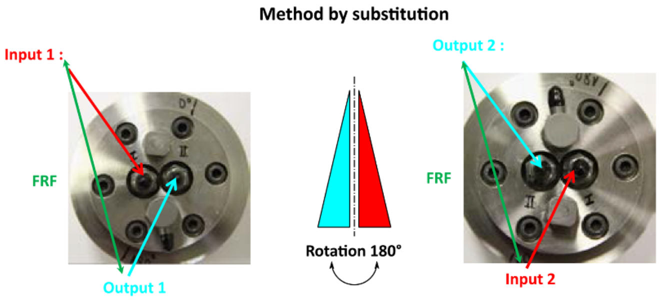

Figure 15. Mounting of the transducer endplate. Configuration A (0°) shown on the left and B (180°) on the right after rotation of the endplate relative to the tube. The FRF calculation configurations for the substitution method are drawn in green.

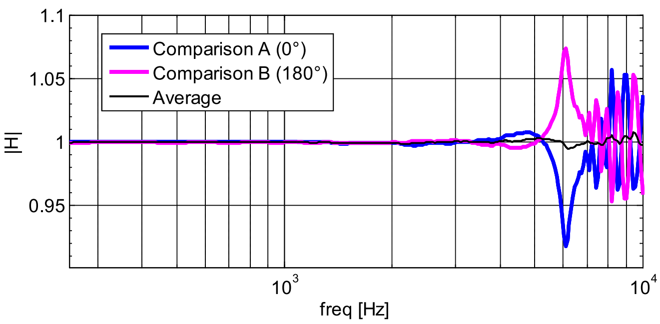

Figure 16. FRFs of measurements based on the reference transducer measurement. Case A (0°) plotted in pink, and case B after 180° rotation in blue. The average, plotted in black, is quasi-flat.

here) also shows that these solicitations are weak compared to the sensitivity to accelerations given by the manufacturer of the pressure transducer. Here these two tests exonerate the accelerations. So in the vicinity of 6 kHz and beyond, the two sensors do not undergo the same pressure; *a priori* this could limit the frequency range useful for calibration by comparison, but a solution is proposed against this.

The origin of the default was studied on the basis of measurement in which the positions of the transducers relative to the tube were exchanged. To do this, the endplate on which the transducers are mounted has been rotated 180° relative to the rest of the tube as shown in figure 15. Case A in the figure is the standard position at 0°, and case B after 180° rotation of the endplate supporting the transducers. In each case the FRFs are calculated on the basis of the signal measured by the reference transducer; the results are shown in figure 16. First of all, it can be noticed that for FRFs that could be used in the process of direct dynamic calibration, the default attributable to the geometric accident inside the tube, which was at 4.5 kHz, disappears. Secondly, the asymmetry observed at 6 kHz and beyond appears more clearly. Consequently, the method may no longer be satisfactory for calibration in the frequency range higher than that of the appearance of this latter default since it abnormally increases the uncertainty of calibration u_{G_c} by more than 7%.

However, the spectral amplification in case A (0°) and case B (180°) appears to be quasi-symmetrical with respect to the gain line $|H| = 1$. The average of the two curves, which is

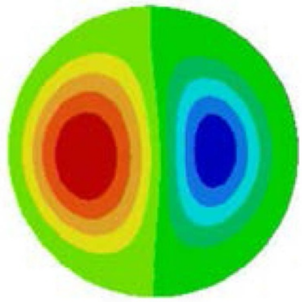

Figure 17. Representation of the shape associated with the first transverse acoustic at the origin of the default. Arbitrary colours are used to represent the mode shape given by an FEM calculation.

almost flat, underlines this point. Thus a transversal acoustical mode of the tube could be suspected of being the cause of the default. Indeed, if the basic theoretical formulation of the first transverse acoustical mode of the tube is taken into consideration (equation (11)), with the speed of sound in the media conditions in domain 2 (see figure 3) of about 360 m s^{-1} and the diameter of the tube $D = 35$ mm, the frequency mode f is of about 6 kHz. The shape of the mode can be represented conventionally according to figure 17, where the results of a calculation carried out according to the finite element method (FEM), and corresponding to the shape of the second mode of a tube in continuous medium, are plotted. Consequently the transducers are not subjected to exactly the same pressure at all time. The phenomenon is naturally compensated for a sensor placed in the centre of the tube by a process of spatial integrations; this is the case in primary calibration.

$$f = 0.585\frac{a}{D} \tag{11}$$

4. Technical propositions for calibration by comparison

If a reference transducer was not used for calibration, each result would depend on the ST used and the particular defaults of the input it produces; the traceability would be lost if this ST and its equipment were not the primary reference. For a secondary calibration the point is that the reference transducer and the transducer in calibration have to be subjected to the same input. So three methods could be used with different levels of performances, as below.

4.1. Ordinary method by direct comparison

For the ordinary direct method, the calibration is carried out from a sequence of measurements where the transducers remain in the standard location (case A, figure 15). A total of four measurements is acceptable to observe a quasi-convergence in repeatability. If this ordinary method is followed, the uncertainty component B2 (experimental deviation) increases considerably at the frequencies of the transversal mode and beyond, because of the effects of the pressure field endplate which is not axisymmetric. The final budget of uncertainty for a calibration by comparison could be two times that of the same kind of transducer calibrated with the primary method in this frequency range (not drawn here). If the objective is to obtain an uncertainty budget which remains reasonably higher than that of the calibration of the reference sensor, the calibration range must be reduced below the frequency of the first transverse acoustic mode of the tube.

Note that if the air used as media can be exchanged by helium, for example, the limitation would be pushed back since the speed of sound is found in the relation, which gives the frequency of the transverse acoustic mode in question. In the case presented before on TCHF dev2.0, the limit of 6 kHz in air would be pushed to 18 kHz in helium.

4.2. Substitution method

This method consists of making the transverse acoustic mode non-observable as is the case for a transducer placed at the centre of the endplate. For this, a series of measurements are carried out in symmetrical ABBA configurations.

The calibration is carried out from two series of measurements; for the first the transducers are placed in the standard locations and for the second their positions are exchanged (case A and case B, figure 15). Thus two series of four measurements are made. For the frequency range below the appearance of the phenomenon there is no change compared to the ordinary method except that more measurements are used. The average of the FRFs is used to define the uncertainty component B2. As previously shown in figure 16, in the frequency range impacted by the phenomenon, the average makes the effect of transverse modes almostnot observable. The variances are considered four by four to recompose the standard deviation used to assess the uncertainty A1 attributable to the repeatability of the eight measurements. The key points of this substitution method are that input and output are measured simultaneously and the FRFs are calculated based on the measurements of the reference transducer; the transducers are not dismounted but the endplate is rotated relative to the tube. Figure 18 shows the budget and the components of uncertainty obtained, and table 2 gives details on the calculation of the uncertainty components. In the end, when the final uncertainty of this secondary calibration is compared with that of the reference transducer with the uncertainty from the reference transducer (‘Rough Uncertainty’ curve and ‘B5’ curve in figure 18), the increase remains acceptable as expected given that the two transducers are equivalent. The method could be used to disseminate a primary using a transducer of the same quality as the reference transducer, and this without having to limit the calibration range because of the transverse acoustic mode of the tube.

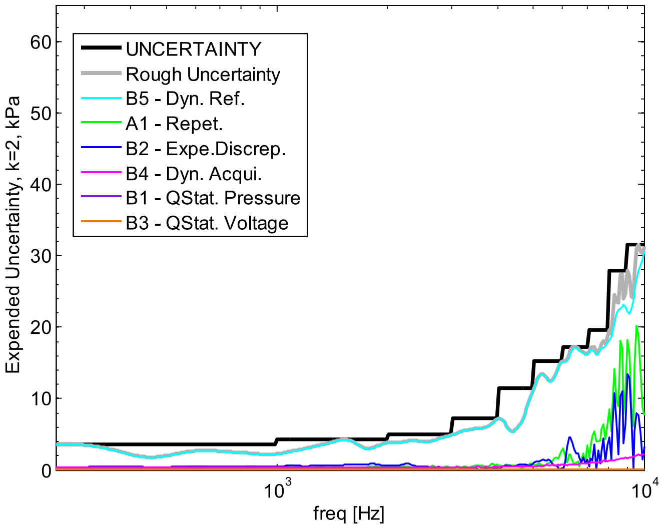

Figure 18. Budget of uncertainties of the secondary dynamic pressure calibration according to the substitution method, in the final step of evaluation. Final result retained is the black curve after the higher values in the sub-frequency ranges have been retained. The raw result is the grey curve. On the plot, all standard uncertainties are multiplied by the factor 2 to allow graphical comparison.

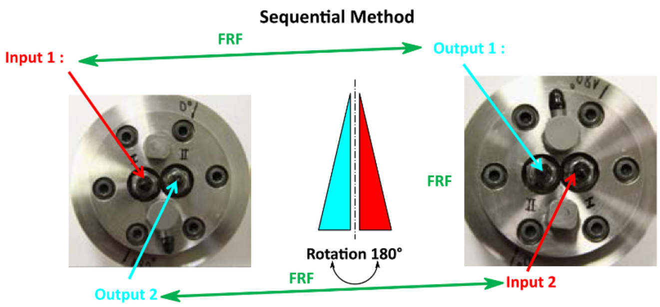

Figure 19. Mounting of the transducer endplate. Configuration A (0 °) shown on the left side and B (180 °) on the right side after rotation of the plate relative to the tube. The FRF calculation configurations for the sequential method are drawn in green.

4.3. Sequential method for validation of substitution method

The sequential method is less satisfactory. It also consists of trying to make the fluctuations of the transverse acoustic mode not observable. The calibration is carried out from two series of measurements where the transducers are first in standard locations and where the positions are exchanged for the second series. FRFs are calculated from input and output measurements taken at the same position relative to the tube. For this the input and output measurements are carried out sequentially, as illustrated in figure 19. Input is measured at one location in series A, and output is measured at the same location in series B. The repeatability of the ST is therefore crucial and has a significant influence on the final result; for this reason this method is not selected for secondary calibration but only used here for the validation of the substitution method. Figure 20 shows the uncertainty budget obtained by the sequential method. Component B2 (which gives the difference to the ideal FRF) is very similar to that obtained with the substitution method; this proves that the substitution method is valid to make the effects of transverse acoustic mode not observable. Component A1 is higher than for substitution

Table 2. Parameters for calculating the uncertainty components involved in the substitution method.

Source	Type	Comment	Distribution
Repeatability	A1	Composition of variances in configuration AB and BA to evaluate the dispersion on the average of samples considered 4 by 4 in frequency domain	$\sqrt{4}$
Dynamic gain	B2	Average of differences between the gain measured and ideal gain ($G_{\_ideal} = 1$). Evaluated for each frequency.	$\sqrt{3}$
Quasi-static sensitivity of the transducer	B1	Quasi-static calibration of the transducer	2
Quasi-static sensitivity of acquisition chain	B3	Quasi-static calibration of the acquisition system	2
Dynamic gain of acquisition chain	B4	Dynamic calibration of the acquisition system. Done with voltage step generators by following an equivalent method as for dynamic pressure.	2
Dynamic gain of reference transducer	B5	Dynamic calibration of the reference transducer	2
Processing	B6	Evaluation of processing of FRF uncertainty. From differences between computational results of time models and their theoretical FRFs (involved in B4); [5] shows quasi-normal distributions	2

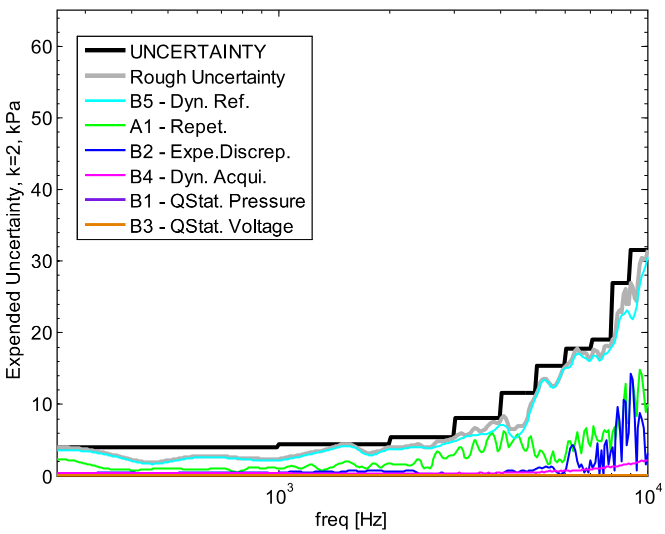

Figure 20. Budget of uncertainties of the secondary dynamic pressure calibration according to the sequential method in the final step of evaluation. Final result retained is the black curve after the higher values in the sub-frequency ranges have been retained. The raw result is the grey curve. On the plot, all standard uncertainties are multiplied by the factor 2 to allow graphical comparison.

measurements, which shows that sequential measurements are subject to the repeatability of the ST.

5. Discussion

The direct method is limited when the transverse acoustic mode of the tube occurs and the sensors are no longer exactly subjected to the same pressure. Substitution is a way to overcome this problem of non-uniformity of the pressure field which appears on the endplate of the ST, while carrying out a calibration by comparison. Here, the shape of the mode has a diametrical symmetry but the method could correct real problems of asymmetry. An alternative is the sequential method where the transducers could be placed in the centre of the tube but sequentially; however, it is not as effective as the previous method due to the repeatability of the shots from the tube.

6. Conclusion

At this stage in the development of calibration methods of pressure transducers in the dynamic regime, which use step generators in a gaseous medium, it seems possible to evaluate the sensitivity of the transducer with an associated uncertainty according to a primary method, and then disseminate it using a secondary method by comparison.

For dissemination it seems possible to use STs which generate steps which are not quasi-perfect, contrary to what is required for primary calibration; however, it is important to check that the sensors are exposed to almost the same pressure.

For the calibration by comparison carried out for this work, the default of the pressure fields identified as coming from a default of internal and axisymmetric inner shape of the tube has no significant effect on the results. However, the default of pressure fields identified as coming from the transverse acoustic mode of the tube can be problematic for calibration in the frequency range in the vicinity and above the mode.

If the objective is to obtain an uncertainty budget which remains reasonably higher than that of the reference transducer, the range of calibration used by ordinary comparison must be reduced below the frequency of the first transverse acoustic mode. Otherwise, the substitution method, which recalls the ABBA method, can be used to make the effect of the transverse acoustic mode not observable. In this case the average of the FRFs is almost the same as the average of the FRFs obtained sequentially when the input and the output are measured in the same location on the tube endplate but not simultaneously. This last result tends to show that the substitution method is acceptable to reduce the effect of the transverse mode of the tube.

Acknowledgements

This project has received funding from the EMPIR programme co-financed by the Participating States and from the European Union's Horizon 2020 research and innovation programme.

ORCID iD

Christophe Sarraf
https://orcid.org/0000-0002-3816-0662

References

[1] ISA-37.16.01 2002 A guide for the dynamic calibration of pressure transducers (ISA) North Carolina

[2] Damion J P 1993 Etalonnage en dynamique des capteurs dans le domaine des basses pressions *6e Congrès Int. de Métrologie, Nîmes, France*

[3] Schweppe J L, Eichberger L C, Muster D F, Michaels E L and Paskusz G F 1963 Methods for the dynamic calibration of pressure transducers *National Bureau of Standards Monograph* **67**

[4] Hjelmgren J 2002 Dynamic measurement of pressure, a literature survey *SP Report 2002: 34, Swedish National Testing and Research Institute*

[5] Olivera A B 2004 Contribution à l'étalonnage dynamique des capteurs de pression. Modélisation de l'incertitude associée *Thèse de l'école doctorale ENSAM Paris* 2004-**30**

[6] Sarraf C and Damion J 2018 Dynamic pressure sensitivity determination with mach number method *Meas. Sci. Technol.* **29** 054006

[7] Saxholm S *et al* 2018 Development of measurement and calibration techniques for dynamic pressures and temperatures (DynPT): background and objectives of the 17IND07 DynPT project in the European metrology programme for innovation and research (EMPIR) *JPhCS* **1065** 162015

[8] Diniz A C G C, Oliveira A B, Vianna J and Neves F 2006 Dynamic calibration methods for pressure sensors and development of standard devices for dynamic pressure *XVIII Imeko World Congress Metrology. Rio de Janeiro, Brazil* vol **2006** pp 17–22

[9] Razzak S, Amaichan J, Damion J P and Sarraf C 2013 Dynamic pressure calibration *The Twenty-third Int. Offshore and Polar Engineering Conf. Int. Society of Offshore and Polar Engineers* vol **2013**

[10] Davis H J and Curchack H D 1969 Shock tube techniques and instrumentation *Harry Diamond Labs Adelphi MD*

[11] Duff R E 1959 Shock-tube performance at low initial pressure *Phys. Fluids* **2** 207–16

[12] Pain H J and Rogers E W E 1962 Shock waves in gases *Rep. Prog. Phys.* **25** 287

[13] Hanson R K and Davidson D F 2014 Recent advances in laser absorption and shock tube methods for studies of combustion chemistry *Prog. Energy Combust. Sci.* **44** 103–14

[14] Theodoro F R F, da Costa Reis M L C, Souto C D A and de Barros E 2016 Measurement uncertainty of a pressure sensor submitted to a step input *Measurement* **88** 238–47

[15] Sembian S and Liverts M 2020 On using converging shock waves for pressure amplification in shock tubes *Metrologia* **57** 035008

[16] Daru V and Damion J P 1995 Analysis of the flow perturbations in a shock tube due to the curvature of the diaphragm *Shock Waves@ Marseille I* vol 1995 (Berlin: Springer) pp 451–6

[17] Glass I I and Hall J G 1959 Handbook of supersonic aerodynamica *Section 18, Shock Tubes, Navord Report 1488* (6 December 1959)

[18] Oppenheim A V and Schafer R W 1989 *Discrete-time Signal Processing* (Prentice Hall) 2nd edn Upper Saddle River, NJ

[19] Betta G, Liguori C and Pietrosanto A 2000 Propagation of uncertainty in a discrete Fourier transform algorithm *Measurement* **27** 231–9

[20] Yao Z, Wang Z, Wang C and Lv J 2018 A fast estimation of shock wave pressure based on trend identification *Meas. Sci. Technol.* **29** 045001